T1- and T2*-Mapping for Assessment of Tendon Tissue Biophysical Properties: A Phantom MRI Study

Bachmann, Elias ; Rosskopf, Andrea B ; Götschi, Tobias ; Klarhöfer, Markus ; Deligianni, Xeni ; Hilbe, Monika ; Pfirrmann, Christian W A ; Snedeker, Jess Gerrit ; Fischer, Michael A

Abstract: OBJECTIVES The aim of this study was to quantitatively assess changes in collagen structure using MR T1- and T2*-mapping in a novel controlled ex vivo tendon model setup. MATERIALS AND METHODS Twenty-four cadaveric bovine flexor tendons underwent MRI at 3 T before and after chemical modifications, representing mechanical degeneration and augmentation. Collagen degradation (COL), augmenting collagen fiber cross-linking (CXL), and a control (phosphate-buffered saline [PBS]) were examined in experimental groups, using histopathology as standard of reference. Variable echo-time and variable-flip angle gradient-echo sequences were used for T2*- and T1-mapping, respectively. Standard T1- and T2-weighted spin-echo sequences were acquired for visual assessment of tendon texture. Tendons were assessed subsequently for their biomechanical properties and compared with quantitative MRI analysis. RESULTS T1- and T2*-mapping was feasible and repeatable for untreated (mean, 545 milliseconds, 2.0 milliseconds) and treated tendons. Mean T1 and T2* values of COL, CXL, and PBS tendons were 1459, 934, and 1017 milliseconds, and 5.5, 3.6, and 2.5 milliseconds, respectively. T2* values were significantly different between enzymatically degraded tendons, cross-linked tendons, and controls, and were significantly correlated with mechanical tendon properties ($r = -0.74$, $P < 0.01$). T1 values and visual assessment could not differentiate CXL from PBS tendons. Photo-spectroscopy showed increased autofluorescence of cross-linked tendons, whereas histopathology verified degenerative lesions of enzymatically degraded tendons. CONCLUSIONS T2*-mapping has the potential to detect and quantify subtle changes in tendon collagen structure not visible on conventional clinical MRI. Tendon T2* values might serve as a biomarker for biochemical alterations associated with tendon pathology.

DOI: https://doi.org/10.1097/RLI.0000000000000532

T1- and T2*-Mapping for Assessment of Tendon Tissue Biophysical Properties
A Phantom MRI Study

Elias Bachmann, MSc,† Andrea B. Rosskopf, PD, MD,‡§ Tobias Götschi, MSc ETH,*† Markus Klarhöfer, Dr Rer Nat,|| Xeni Deligianni, PhD,¶# Monika Hilbe, Dr Med Vet,** Christian W.A. Pfirrmann, MD exec MBA UZH,‡§ Jess Gerrit Snedeker, PhD,*† and Michael A. Fischer, PD, MD‡§*

Objectives: The aim of this study was to quantitatively assess changes in collagen structure using MR T1- and T2*-mapping in a novel controlled ex vivo tendon model setup.

Materials and Methods: Twenty-four cadaveric bovine flexor tendons underwent MRI at 3 T before and after chemical modifications, representing mechanical degeneration and augmentation. Collagen degradation (COL), augmenting collagen fiber cross-linking (CXL), and a control (phosphate-buffered saline [PBS]) were examined in experimental groups, using histopathology as standard of reference. Variable echo-time and variable-flip angle gradient-echo sequences were used for T2*- and T1-mapping, respectively. Standard T1- and T2-weighted spin-echo sequences were acquired for visual assessment of tendon texture. Tendons were assessed subsequently for their biomechanical properties and compared with quantitative MRI analysis.

Results: T1- and T2*-mapping was feasible and repeatable for untreated (mean, 545 milliseconds, 2.0 milliseconds) and treated tendons. Mean T1 and T2* values of COL, CXL, and PBS tendons were 1459, 934, and 1017 milliseconds, and 5.5, 3.6, and 2.5 milliseconds, respectively. T2* values were significantly different between enzymatically degraded tendons, cross-linked tendons, and controls, and were significantly correlated with mechanical tendon properties ($r = -0.74$, $P < 0.01$). T1 values and visual assessment could not differentiate CXL from PBS tendons. Photo-spectroscopy showed increased autofluorescence of cross-linked tendons, whereas histopathology verified degenerative lesions of enzymatically degraded tendons.

Conclusions: T2*-mapping has the potential to detect and quantify subtle changes in tendon collagen structure not visible on conventional clinical MRI. Tendon T2* values might serve as a biomarker for biochemical alterations associated with tendon pathology.

Key Words: bovine flexor tendon, magnetic resonance imaging, T1-mapping, T2*-mapping, biomechanics, tendinopathy

(*Invest Radiol* 2018;00: 00–00)

The Achilles tendon and its enthesis (attachment at the bone) enable the mechanical force transmission from the calf muscles to the heel and are therefore important biomechanical structures for plantar flexion of the foot. The major component of tendon dry weight is collagen type I (65%–87%), embedded in a noncollagen extracellular matrix that mainly consists of water and small leucine-rich proteoglycans with glycosaminoglycan (GAG) side chains.[1,2] This extracellular matrix undergoes increasing disorganization with advancing stages of tendon disease, with concomitant loss of mechanical integrity[3–6] and change in water permeability.

Magnetic resonance imaging (MRI) is commonly used for assessing tendon disease based on qualitative morphologic criteria, but interrater reliability varies substantially ranging from moderate to excellent.[7–9] Moreover, sensitivity of standard turbo spin-echo T1- and T2-weighted sequences for early tendon degeneration is limited by the short T2 MR characteristics by highly organized tendon tissue components. Because tendons have a characteristically short T2 signal, use of standard MR sequences results in poorly visualized tendon structures in both healthy and slightly degenerated Achilles tendon.[10]

With ultrashort echo-times pulse sequences, it is possible to gain signal from tissues characterized by a short T2 time (such as tendons) before complete signal decay.[11,12] Alternatively, manipulated variable echo-time sequences have been shown to be useful for visualization and quantitative assessment of fast-relaxing tissues, providing high image quality at 3 T and T2*-mapping with very-short echo-times below 1 millisecond.[13–16] The short T2* component of the tendon is thought to represent water protons bound to macromolecules such as GAGs, whereas the long T2* component is associated with the free water content of the tendon.[17] During tendon cross-linking, which is associated with tendon aging and early tendon degeneration,[11] changes in tendon structure lead to a shift from free to macromolecule bound water molecules, whereas proceeding tendon degeneration leads to collagen disruption and an increase of the free water content. The relation of bound versus free water protons associated with different tendon collagen structures[18] might be detected and quantified by T2*-mapping of short echo-times[17] and might therefore serve as a biomarker for collagen degradation.[19]

Detection of changes within pathological tendons in the absence of early morphological changes on standard imaging could plausibly provide clinical benefit, for instance, in the prescription of prophylactic physiotherapy to mitigate disease progression before the onset of deeper structural damage.[20]

The aim of the present study was to implement a phantom model for quantitative assessment of changes in tendon structure and mechanical function. Ultimately our goal was to quantitatively assess the potential for reliably detecting changes in the physical collagen matrix of tendon tissue using T1- and T2*-mapping. We tested this using healthy, enzymatically degraded and augmented bovine flexor tendons, placing the MR measurements in context of histological and mechanical changes induced by the tissue alteration.

MATERIALS AND METHODS

Study Design

Three experimental groups, each with 8 tendons, were investigated by MRI. The experiment was performed at 2 different time-points (Fig. 1).

Received for publication September 11, 2018; and accepted for publication, after revision, October 5, 2018.

From the *Department of Orthopedics, Balgrist University Hospital; †Institute for Biomechanics, Swiss Federal Institute of Technology in Zurich; ‡Department of Radiology, Balgrist University Hospital; §University of Zurich, Faculty of Medicine; ||Siemens Healthcare AG, Zurich; ¶Division of Radiological Physics, Department of Radiology, University Hospital of Basel, University of Basel, Basel; #Department of Biomedical Engineering, University of Basel, Allschwil; and **University of Zurich, Institute of Veterinary Pathology, Zurich, Switzerland.

Conflicts of interest and sources of funding: none declared.

Correspondence to: Elias Bachmann, MSc, Balgrist Campus, Lengghalde 5, 8008, Zurich, Switzerland. E-mail: elias.bachmann@balgrist.ch.

ISSN: 0020-9996/18/0000–0000
DOI: 10.1097/RLI.0000000000000532

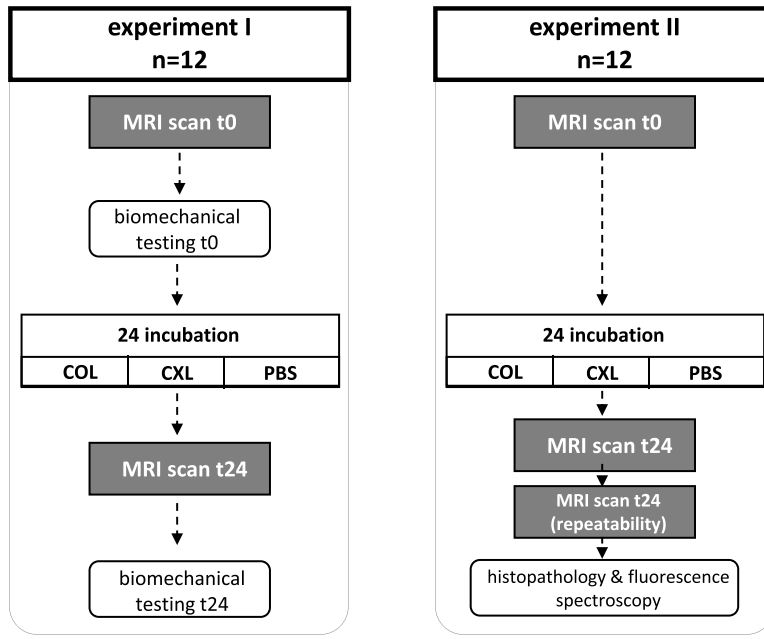

FIGURE 1. Flowchart of the 2 experiments with each 3 groups (collagenase [COL], collagen cross-linked [CXL], or phosphate-buffered saline [PBS]). Although biomechanical properties were investigated during experiment I, test-retest reliability of the setup, histophatology, and fluorescence spectroscopy were performed in experiment II. MRI scan t0 is the initial scan and t24 the scan after 1 day of incubation of samples. To asses reproducibility of the scans using this setup, experiments I and II were performed between 4 weeks' time difference.

Half of all tendons were assessed by destructive biomechanical testing, and the other half were processed for histological analysis.

To obtain a reproducible model with variable mechanical properties of a tendon, which reflect degenerative changes in the diseased collagen matrix, we targeted the mechanical properties of the tendon with biochemical substances. It is well known that collagen cross-linking agents affect the tendon's elastic (ie, elastic modulus) and viscoelastic (ie, stress-relaxation) behavior,[3,21] and elevated tissue cross-linking has been increasingly associated with tendon scarring, diabetic tendinopathy, and inflammatory connective tissue disease.[22] A denser collagen interconnection, induced by cross-linking, also results in a decreased matrix porosity, which consequently will result in reduced water movement. Correspondingly collagenase treatment tends to increase porosity and results in less constrained tissue water movement. Collagenase also affects the tendon's elastic behavior[23] and leads to a degenerated tendon tissue in a concentration- and time-dependent fashion by disrupting their collagen continuity.

After an initial image acquisition of yet untreated specimens, 0.2 mL of different solutions were injected with a 24-gauge cannula or gauge needle directly in the middle portion of the respective tendon. In the control group, phosphate-buffered saline (PBS) was injected. For the 2 interventional groups, either collagenase B (COL; 0.226 U/mg lyo; PBS with Ca2+) with a concentration of 12 mg/mL or a collagen cross-linking (CXL) solution (2 mL, 80 mM genipin in PBS and 2% DMSO) with a concentration of 80 mM was infiltrated.

After a second scanning run, the MRI clamping device was then stored at 37°C in an incubator after wrapping all tendons in saline-soaked gauzes and sealing them tightly to prevent dehydration. After 24 hours, tendons were then scanned again.

Immediately after the final scan, tendons were removed from the clamping device and either analyzed biomechanically or histologically to assess the effects of the imposed chemical treatment.

Phantoms

For this study, 12 bovine flexor tendons with an average cross-sectional area of 20 mm^2 were obtained freshly from a local abattoir (Metzgerei Angst, Zurich, Switzerland). Immediately after purchase, the tendons were prepared by removing synovial lining and unnecessary soft tissue. Tendons were cut in half (8 cm) and randomly assigned into 3 groups while they were covered in saline-soaked gauze to avoid sample dehydration. To ensure a reproducible testing environment, tendon specimens were mounted on a 3-dimensional printed custom-made MRI compatible clamping device, placed in a plastic container and filled with PBS. The container was then sealed airtight with its lid and positioned horizontally into the detector reel, so that tendons were oriented perpendicular to the axis of the main magnetic field (Fig. 2).

Magnetic Resonance Imaging

Magnetic resonance imaging was performed on a 3 T MRI system (MAGNETOM Skyra; Siemens Healthcare, Erlangen, Germany) using a dedicated knee coil. The MRI study protocol consisted of the standard clinical MRI protocol at our department for the examination of the Achilles tendon as well as T1- and T2*-mapping sequences, which were optimized for imaging of tissues exhibiting short T2* values. A variable flip-angle gradient-echo sequence using short radiofrequency excitation pulses and short echo-times was used for T1-mapping. For T2*-mapping, a variable echo-time sequence[13,14] consisting of a series of 4 multiecho gradient-echo acquisitions each collecting 5 echo images. For the complete multiecho acquisition, the first echo time was variable[14] and the 5 echo-train was sequentially shifted to obtain a series of 20 gradient echo images with an echo spacing of 1 millisecond. The imaging protocol and corresponding imaging parameters are displayed in Table 1.

MRI Data Analysis

T1 values were calculated by the software of the MR system by pixel-wise fitting of the signal intensities obtained at different flip angles to the signal equation of a spoiled gradient echo sequence. T2*-map calculation was performed in Matlab (The MathWorks Inc, Natick, MA), assuming a monoexponential decay of the measured signal intensity S(TE).

T1 and T2* isotropic maps were reformatted in the transverse plane with a slice thickness of 10-mm centered on the injection site at the middle of the tendons (Fig. 3). Two independent readers (one

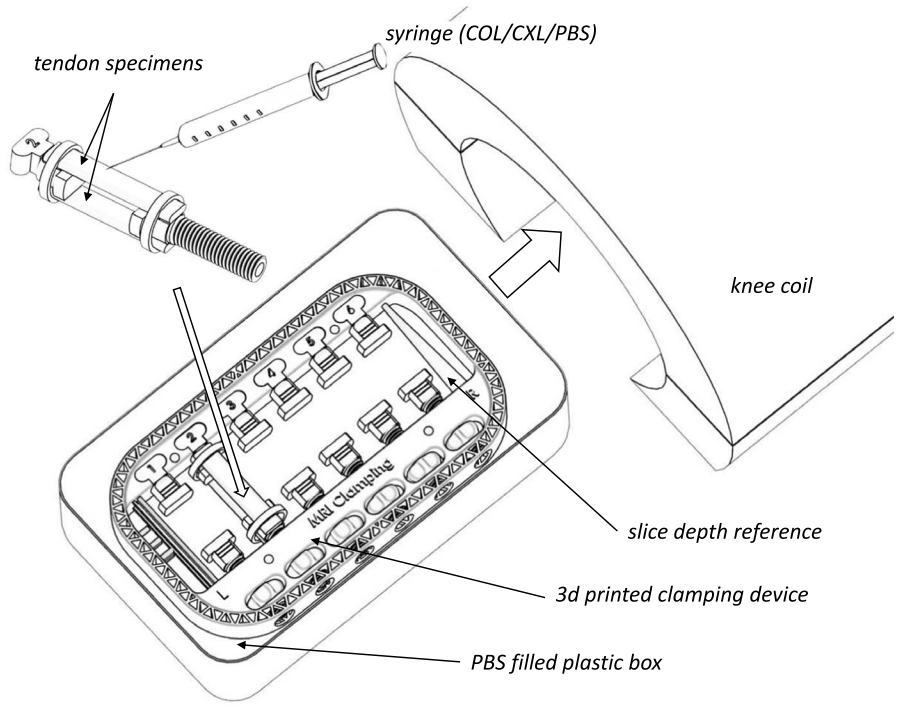

FIGURE 2. Experimental setup: custom-made clamping device with 12 tendon samples rigidly mounted in a plastic box (6 up, 6 down), filled with PBS solution during scans. Collagenase (COL), a cross-linking agent (CXL), or phosphate-buffered saline (PBS) was injected in the tendons to obtain 2 groups undergoing a chemical change in tendon structure and one serving as a control group (PBS).

musculoskeletal radiologist with 6 years of experience, one MRI physicist with 10 years of experience) evaluated the images. Image analysis was fully blinded with respect to specimen grouping, as was analysis of biomechanical test results, and histopathological grading. Imaging datasets were evaluated using T1-mapping and T2*-mapping images with designated ROI implemented freehand along the transverse plane of each tendon and spanning the maximum tendon diameter but avoiding the interface between tendon and surrounding water.

T1 and T2* times were assessed separately for untreated and treated tendons and corresponding percentage differences (Δ) of T1 and T2* times were calculated between matched treated and untreated tendons according to the following algorithm: $\Delta_{T1/T2*}$ = (treated − untreated)/untreated × 100 (%).

As T1 and T2* values and scaling differ in absolute numbers, percentage difference were calculated to better compare relative difference each treatment induced compared with the untreated tendons.

Qualitative Analysis of MRI Data

Two musculoskeletal radiologists (each 6 years of experience), who were blinded to the test condition and all other results, performed standard qualitative clinical analysis. Quality of the bovine tendon was visually assessed before and after treatment using standard T1-weighted and STIR (short tau inversion recovery) images in the coronal plane according to the clinically implemented protocol of the institution.

In this musculoskeletal imaging center, STIR images are implemented in clinical routine for T2-weighted fat suppression to achieve more homogeneous fat suppression.

All images were interpreted on a standard workstation using an integrated picture archiving and communication system (IMPAX 6, Agfa HealthCare, Bonn, Germany).

Quality of the bovine tendon was rated on a 4-point scale with the following specifications: 0, "normal tendon," no T1-/STIR signal alterations; I, "edema," hyperintense areas on T1-weighted images; II, "partial tear," hyperintense on STIR-weighted images; and III, "complete tear," discontinuity of the tendon.

Biomechanical Testing of Tendons

For experiment I, all 12 tendons were tested before and after incubation in a calibrated and certified uniaxial universal material testing machine (Zwick 1456; Zwick GmbH, Ulm, Germany). After applying a preload of 10 N, tendons were stretched to a strain of 5% and the exerted

TABLE 1. MR Protocol (3 T, SkyraFit)

Parameters	Morphologic		T1-Mapping	T2*-Mapping
Sequence	T1w-TSE	STIR T2w-TSE	Variable Flip Angle GRE	Multiecho GRE
Dimensions	2	2	3	3
Voxel dimensions, mm^3	0.5 × 0.5 × 3	0.5 × 0.9 × 3	0.8 × 0.8 × 0.8	1 × 1 × 1
Repetition time, ms	680	4500	15	32
Echo time, ms	11	44	1.8	1, 2, 3,…, 20
Flip angle, degrees	90	90	6, 19, 33	8
Bandwith, Hz/Pixel	255	245	430	320

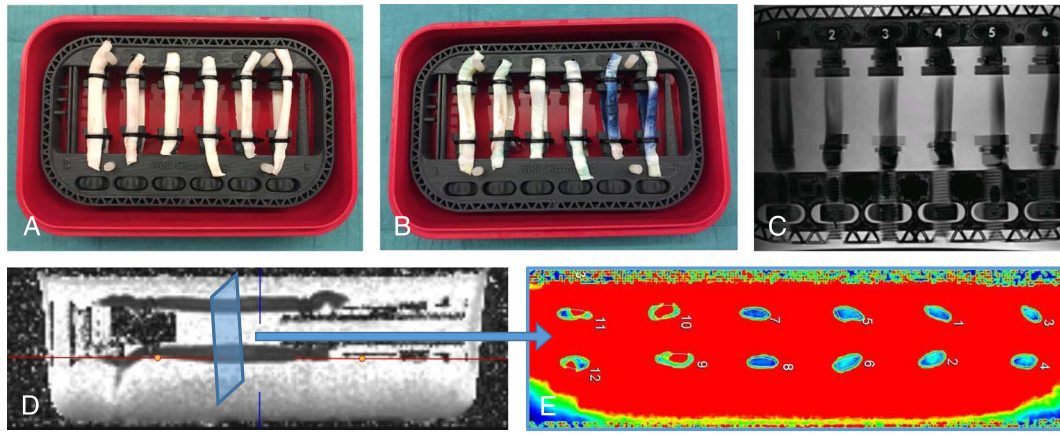

FIGURE 3. Before (A) and after 24 hours (B) of incubation of treated tendons. Image C shows a standard T2-weighted sequence-slice of the posttreated phantom. D, Side view with indicated axial plane (blue plane). E, Visual example of T1 color map for data read out in axial orientation.

force was recorded. Measurement of tendon stress at small strain levels (≤5% strain) allows to obtain mechanical data of differently treated tendons while keeping the microstructure of the tendon intact. For stress calculation, the cross-sectional area of the tendon specimen was scanned in triplicate using a custom made linear laser measurement device (accuracy, −3.52% ± 1.89%; precision, 0.83%).[24,25]

Histopathology and Immunohistology of Tendons

In experiment II, tendons used for histopathology analysis were cut in 3 pieces. The distal and medial (middle) portions were then stored in CryoTubes and filled with formaldehyde solution 4%, ph 7, buffered (Roti-Histofix, Carl Roth GmbH, Germany).

After fixation, the tendons were cut into a longitudinal and 2 cross-sections before they were routinely embedded into paraffin. Cut sections of 2- to 3-µm thickness were afterward sectioned and stained with hematoxylin and eosin. Unstained paraffin-embedded tendon sections were deparaffinized and the antigen demasked by boiling the slides in a pressure cooker (Pascal, DakoCytomation) at 80°C in a basic buffer. Afterward, the tendons were incubated for 1 hour at 37°C with the polyclonal rabbit anti-collagen I antibody (Abcam Ab34710) at a dilution of 1:100. As secondary antibody, the Red Map Kit (760–4154 Roche [rabbit/mouse]) was used and then the slides evaluated by light microscopy.

Collagen cross-linking was verified by making use of its distinct optical spectral properties. Genipin cross-links emit fluorescence at a peak wavelength of 630 nm when excited at 590 nm.[26,27] Microscopy imaging was performed using an inverted spinning disc confocal microscope (iMic; FEI Munich GmbH, Hillsboro, OR) with a 4x N.A. 0.16 objective (Olympus UPlanSApo) and a Hamamatsu Orca-flash 4.0 Digital CMOS camera (C11440-22CU). A collagen exciting wavelength of 405 nm[22] and a genipin-specific wavelength of 560 nm were used for visualization. Histological tendon sections of the control (PBS) as well as CXL treatment group were mounted on a microscope slice and the unstained slides imaged at one z-plane. Image analysis was done in ImageJ (NIH Image). The ratio of mean pixel intensity between both excitation wavelengths was subsequently compared between PBS and CXL sections using Student *t* test (n = 6).

Statistical Analysis of T1 and T2* Maps

The data were descriptively reviewed and statistically tested for normality with the Kolmogorov-Smirnov test. All results were expressed as means ± standard deviations. For quantitative analysis, Student *t* test for not related samples was used to test for significant differences between different groups of tendon preparation. Fisher exact test was used for qualitative visual data analysis, whereas Mann-Whitney *U* test was used to evaluate significant differences of tendon quality. *P* values less than 0.05 were considered statistically significant. All statistical analyses were performed using commercially available software (SPSS, release 20.0, Chicago, IL).

RESULTS

Quantitative Analysis and Percentage Difference in Signal (Pre vs Post)

There was a significant difference of T1 and T2* times between untreated and treated tendons in total (both, $P < 0.001$) and for each group of treatment (COL/CXL/PBS) separately (all, $P < 0.04$, data not shown). Overall, there was an increase in T1 and T2* relaxation times for each group after incubation, whereas the COL group (porosity increasing) showed almost 200% increase of percentage difference (ΔT1 median, 188%; ΔT2* median, 195%).

However, ΔT1 and ΔT2* showed only significant differences between collagenase-treated tendons and both cross-linked and control tendons but not between cross-linked and control tendons ($P > 0.9$, $P = 0.051$; Fig. 4).

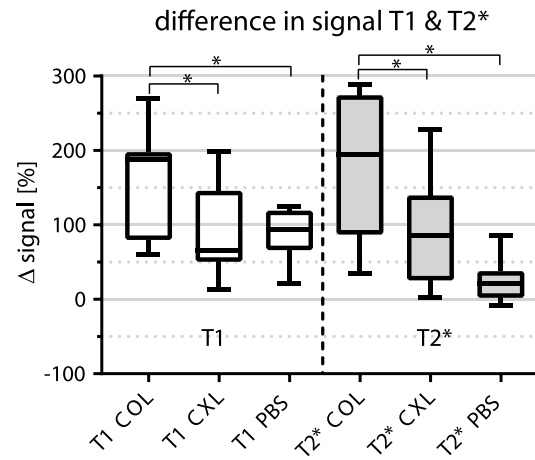

FIGURE 4. Relative difference in T1 and T2* relaxation times of untreated and treated groups: collagenase (COL), collagen cross-linked (CXL) and control (PBS). Boxplots with median and whiskers from minimum to maximum, level of significance is defined as follows: $*P < 0.05$. $\Delta_{T1, T2*}$ = (treated − untreated/untreated).

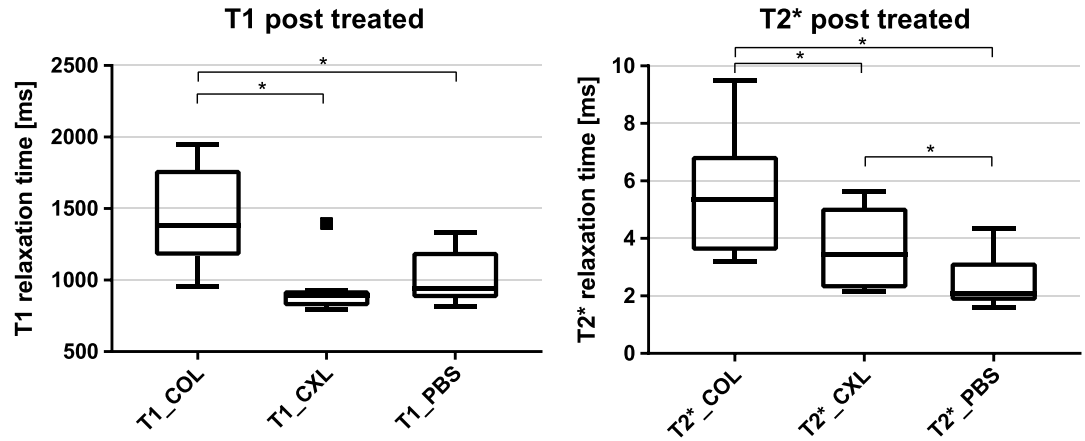

FIGURE 5. T1 and T2* relaxation times of treated groups: collagenase (COL), collagen cross-linked (CXL), and control (PBS). Boxplots with median and whiskers from minimum to maximum, level of significance is defined as follows: $*P < 0.05$.

After Treatment

For T1-mapping (T1_treated), there was a significant difference between COL-treated tendons (median, 1384 milliseconds) showing almost one third higher T1-relaxation times and both CXL-treated (median, 890 milliseconds) and control tendons (PBS; median, 942 milliseconds; all, $P < 0.01$), whereas no significant difference was seen between CXL and PBS-treated tendons (T1 post, $P > 0.3$).

T2* mapping (T2*_treated) revealed significant differences between COL (median, 5.35 milliseconds) and both CXL (median, 3.44 milliseconds) and PBS (median, 2.10; both, $P < 0.01$), as well as between CXL and PBS groups (Fig. 5).

Reproducibility and Repeatability of the Setup

No significant differences of T1 and T2* times were seen between scans of experiment I and experiment II of untreated tendons (both, $P > 0.45$; Fig. 6). For treated tendons, no significant differences of T1 and T2* times were seen between repetitive T1 and T2* scans of experiment II (both, $P > 0.5$).

Results Biomechanics

Before incubation, there was no significant correlation between tendon stress at 5% strain and T2* relaxation time ($P = 0.22$) with an overall mean value of 13.14 ± 5.6 MPa at 5% strain. However, after treatment of tendons, a significant linear regression emerged ($r = -0.74$, $P < 0.01$), indicating that treatment agents effected tendon mechanics respective their collagen structure (Fig. 7). Both treatment groups COL and CXL showed a decrease in stress (−49%, −14%) at 5% strain, compared with the control group (PBS). Mean stress values for COL-, CXL-, and PBS-treated tendons at 5% strain were 5.0 ± 2.3, 8.5 ± 3.0, and 10.1 ± 3.0 MPa, respectively. For T1-mapping, no significant correlation was seen (data not shown).

Qualitative Analysis by Qualitative, Standard Clinical Analysis of MRI

Both readers clearly identified all COL-treated samples as showing visually detectable degenerative changes (grade II 8/8). In the CXL group, no degenerative changes were noted for both readers, but one tendon demonstrated a visible edema associated with the bolus injection for reader 1 (grade 0, 7/8; grade I, 1/8), whereas reader 2 detected 2 CXL-treated tendons with increased signal on STIR imaging (grade 0, 6/8; grade I, 2/8). Similarly, in the PBS group, no degenerative changes were detected, but 2 tendons were identified with visibly increased water content by reader 1 (grade 0, 6/8; grade I, 2/8), whereas 3 tendons were identified by reader 2 (grade 0, 5/8; grade I, 3/8). Thus, no significant differences in visual evaluation of the CXL and PBS groups were detectable by standard evaluation of the MRI scans for both readers (both, $P < 0.001$).

Results Histopathology and Immunohistology

Visual inspection of CXL-treated tendon samples before histology showed a bluish change in color, whereas COL-treated samples seemed to look more aqueous.

In the tendons treated by collagenase, hematoxylin and eosin staining indicated revealed rounding of cell nuclei, ruptured collagen

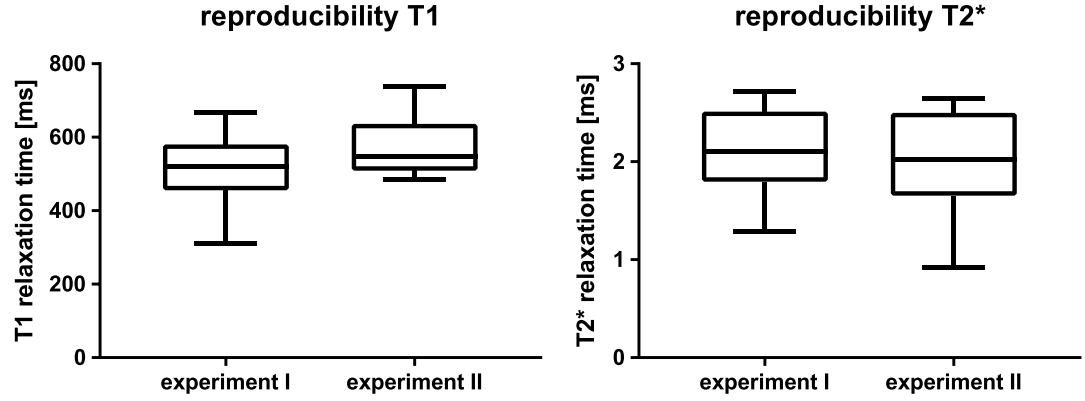

FIGURE 6. Reproducibility of the measurement setup between 4 weeks of experiment 1 and 2 (T1, T2* relaxation times of each 12 tendon specimen before treatment). Boxplots with median and whiskers from minimum to maximum, level of significance is defined as follows: $*P < 0.05$.

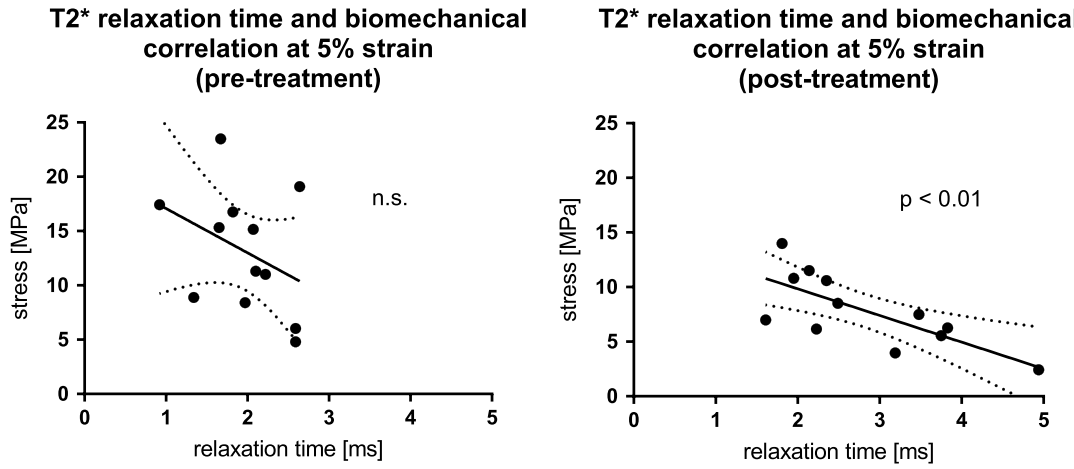

FIGURE 7. T2* stress relaxation and correlation of tendon stress at 5% strain. Black dotted lines indicate the 95% confidence intervals. Left, nonsignificant correlation before treatment. Right, Linear regression of T2* times of treated tendons with relaxation times of treated tendons ($P < 0.01$) and a correlation cofficient of $r = -0.74$.

fibers, and loss of staining intensity (Fig. 8). Collagen I immunohistology also showed less intense staining in the degenerating regions of the collagenase-treated tendons. In contrast, cross-linked tendons showed no observable histological abnormalities or regional variations in collagen staining.

Successful collagen cross-linking by the injected genipin solution was indicated by a measured significant differences in tissue autofluorescence at genipin-specific excitations (Fig. 9).

DISCUSSION

In this study, we implemented a reproducible tissue-based MRI phantom model to test the potential of T1- and T2*-mapping for quantification of biophysical differences in tendon structure and function induced by a range of chemical treatments.[3,28–31] Treated tendons were referenced against benchtop measures of tissue biomechanics and tissue histology. Our results indicated that T1-mapping and T2*-mapping were both capable of detecting collagenase-induced tendon degeneration that resembled advanced stage tendinopathy collagen distortion. Subtle changes with increased tendon cross-linking, however, could be successfully detected using T2*-mapping with short echo times. Interestingly, biomechanical testing correlated exclusively and negatively with T2*-mapping as T2* times and extracellular water content decrease when tendon stress exertion increases.

Conventional MRI shows a limited diagnostic capability for chronic tendinopathy due to intermediate to long echo-times (20–60 milliseconds) of standard spin and gradient echo sequences, which are substantially longer than the intrinsic T2 and T2* values of tendons, which are in the order of a few milliseconds.[32] For this specific application, recently introduced ultrashort echo-times imaging, however, was shown to overcome the limitations of standard sequences allowing visualization and quantification of pathological changes in the human Achilles tendon.[33] For T2*-mapping, a 2-component model reflective of short and long echo-times was proposed. The short component of T2* decay, which is related to bound water of collagen, GAG, and other proteins, allows best for discrimination of healthy from diseased tendons, suggesting that it reflects the changes in water content and collagen orientation more accurately than the long component of T2* decay or T1-mapping, which are related to free water of the interstitial space.[34]

Several studies have been performed assessing relaxation times of healthy and degenerated tendons in vivo and in vitro using T2* with short echo-times.[9,13,33,35–40] Our results in healthy bovine tendons are comparable to T1 and T2* values of a recent ex vivo[34] and in vivo studies,[33,36] with T2* values ranging from 0.92 to 2.72 milliseconds and T1 values ranging from 311 to 733 milliseconds.

There are many factors that can affect T1 and T2/T2* measurements. Although saline solution is recommended to prevent specimen

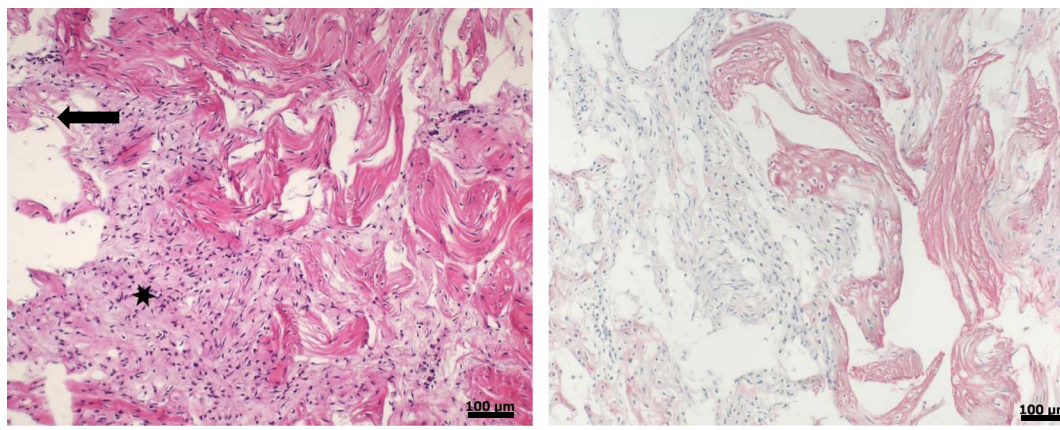

FIGURE 8. Left, hematoxylin and eosin (arrow, degenerating nuclei; asterix, degenerating collagen fibers); on the right and upper side, the collagen fibers are histologically normal. Right, immunohistology collagen I; on the left side, the degenerating collagen fibers show lesser intensity of staining for collagen I compared with the fibers on the right side without histological degeneration signs.

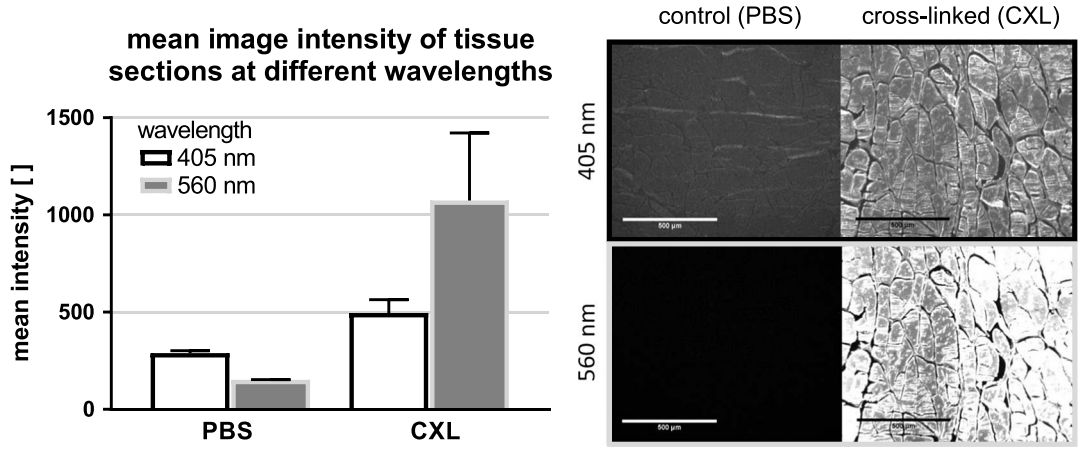

FIGURE 9. Left, Mean image intensity at 405 and 560 nm wavelength of 6 untreated (PBS) and 6 cross-linked (CXL) tissue sections (error bar, ± SD). Right, Confocal images of untreated (left row) and cross-linked (right row) tendon sections. Genipin cross-linked samples show increased fluorescence at 560 nm (lower row), whereas untreated samples show a reduction in fluorescence intensity. All images are displayed at equivalent brightness scale. White respective black bar indicate a length of 500 μm.

dehydration[36] and to minimize susceptibility effects, a study by Zheng and Xia[35] reports that saline and PBS solution have different effects on outcome of T2/T2* values. Moreover, T2/T2* times of water nuclei of tendon tissue is dependent on temperature and the orientation of the tissue relative to the static magnetic field B0.[41–44] Assuming sufficient signal-to-noise ratio, the orientation of the tendons with respect to the main magnetic field does not influence the T1 maps. However, the effective transversal relaxation time T2* depends on the spatial orientation of the tendons with respect to the main magnetic field due to dipolar interactions. Accordingly, we kept temperature and orientation (fiber alignment) of tendons constant (perpendicular to B0) and only immersed tendons in PBS during scanning of samples.

Spatial resolution was adapted to the size of the tendons used in our study and the size of the clamping device. Depending on available signal-to-noise ratio and measurement time, higher spatial resolutions are possible, which could be useful in assessment of smaller tendons.

The influence of magic-angle effects requires further investigation, as do effects associated with imaging tendons of larger and smaller diameter.

In our study, we aimed to evaluate the effect of change in collagen structure on relaxation times in a controlled phantom setting. We chose to investigate alterations to the tendon core collagen structures that are likely to be most reliably discernable by MRI (as opposed to thin structures such as the peritenon).[18] Tendon aging, which refers to the "first" step of tendon degeneration, is characterized by an increase of intercollagen cross-links, as well as increased presence of proteoglycans and other macromolecules.[3] Accordingly, in this "early" stage of tendon degeneration, collagen orientation and water content changes, whereas the tendon structure remains intact. In later stages of tendon degeneration, microtears and degradation can result in collagen distortion with areas of mucoid or fatty degeneration in tendon tissue.[3] Genipin is a chemical agent, which was shown to induce collagen cross-linking in previous in vitro studies,[3,25,45] serving as a general model of collagen cross-linking and biophysical effects associated with decreased porosity and decreased mobility of water within the tissue. The effect of tendon treatment with genipin was visible by a slight blueish coloring of the tendons and confirmed by confocal microscopy serving as the reference standard for increased cross-linking. In comparison, severe tendon degeneration as induced by collagenase showed collagen degradation with increased tissue porosity as assessed using histopathological and biomechanical analysis, respectively. Although the simplified models of degeneration and cross-linking are both nonphysiological, they mimic biophysical changes in tissue structure and function that are hallmarks of disease. Further, they are reproducible, and thus well suited for pilot testing of new radiological test phantoms and methods.[3,23,25,45,46]

When comparing healthy and severely degenerated tendons, several in vivo studies have reported a significant increase in T2 and T2* in degenerative tendon tissue.[47–49] This is consistent with our results showing a significant increase of both T1 (+188%) and T2* (+195%) values in higher degree of tendon degeneration with chemically (collagenase) induced collagen distortion. When comparing healthy and tendons with increased cross-linking, our results showed significantly longer T2* times (+86%) of those functionally modified tendons, whereas T1-mapping and visual analysis failed to distinguish both groups. A noticeable small range of T1 values was observed for the CXL-treated tendons. We hypothesize, as T1 is assumed to reflect (only) the extracellular fluid, which decreases after treatment by CXL, that T1 values decrease compared with the control group and consequently are narrower in range. However, differences were not significant to the control group, which indicated increased presence of extracellular fluid.

The present quantitative and highly controlled work tend to support previous in vivo studies, such as those showing that T2* relaxation times in healthy runners are significantly longer when compared with a normal population (mean percentage increase, 15.7% ± 4.9%),[33] which might be as well explained by an adaption of the tendon matrix (cross-linking) and consecutive changes in the free and/or bound water fractions without patients being symptomatic.

Biomechanical testing correlated exclusively and negatively with T2*-mapping. Accordingly, T2* times increase when tendon stress decreases, which might reflect the increase of extracellular water fraction from cross-linked tendons to collagenase-treated tendons.

Several limitations need to be acknowledged. First, tendons and ligament properties are highly complex, and effects that lead to pathological changes are manifold.[50] In this study, we investigated distinct biophysical changes to the collagen matrix in a controlled phantom and attempted to correlate MRI metrics to histopathological and biomechanical metrics. Although chemical treatments used in this study are both nonphysiological, they are among the best-established means of altering mechanical properties and useful for locally altering tissue function of a phantom in a controlled and reproducible manner.[3,23,25,45,46] Moreover, we did only perform T1- and T2*-mapping using a 3 T system. However, in this pilot study, we aimed to establish a phantom model of collagen degradation allowing for standardized ex vivo evaluation of tendon biomechanics and MRI properties. Finally, the experimental setup was reproducible between scans (experiments I and II)

of untreated tendons and test-retest reliability (experiment II), proving a standardized workflow and reliable setup. However, to improve workflow and optimize a standardized treatment, tendon incubation in a water bath should be considered, to equally effect tendons, which might be more consistent compared with the needle injection applied in this study. Investigation of larger diameter tendons like the human Achilles (60 mm^2 at its smallest cross section, 120 mm^2 at its largest)[51] should be considered for future experiments. However, the authors assume that if biophysical properties are detectable in smaller tendons, they should be even more likely to be reliably quantified in larger diameter tendons.

CONCLUSIONS

A tendon model within a novel, highly controlled setup was successfully introduced in MRI testing environment. Optimized T2*-mapping was inversely and significantly correlated to mechanical function in a range of in vitro experiments on tendons treated by compounds that affect their structure and function. T2* may offer increased potential to detect and quantify early functional changes in collagen structure as it is present in early tendon degeneration before they are visible in standard T1 MRI scans.

ACKNOWLEDGMENTS

The authors thank PD Dr Daniel Nanz, head of the Swiss Center for Musculoskeletal Imaging at Balgrist Campus, for his valuable input and expertise in questions regarding MRI physics in biological tissues.

REFERENCES

1. Kannus P. Structure of the tendon connective tissue. *Scand J Med Sci Sports*. 2000;10:312–320.
2. Kjaer M. Role of extracellular matrix in adaptation of tendon and skeletal muscle to mechanical loading. *Physiol Rev*. 2004;84:649–698.
3. Fessel G, Gerber C, Snedeker JG. Potential of collagen cross-linking therapies to mediate tendon mechanical properties. *J Shoulder Elbow Surg*. 2012;21:209–217.
4. Scott JE. Extracellular matrix, supramolecular organisation and shape. *J Anat*. 1995;187(Pt 2):259–269.
5. Riley G. The pathogenesis of tendinopathy. A molecular perspective. *Rheumatology (Oxford)*. 2004;43:131–142.
6. Docking S, Samiric T, Scase E, et al. Relationship between compressive loading and ECM changes in tendons. *Muscles Ligaments Tendons J*. 2013;3:7–11.
7. Fischer MA, Pfirrmann CW, Espinosa N, et al. Dixon-based MRI for assessment of muscle-fat content in phantoms, healthy volunteers and patients with achillodynia: comparison to visual assessment of calf muscle quality. *Eur Radiol*. 2014;24:1366–1375.
8. Tsehaie J, Poot DHJ, Oei EHG, et al. Value of quantitative MRI parameters in predicting and evaluating clinical outcome in conservatively treated patients with chronic midportion Achilles tendinopathy: a prospective study. *J Sci Med Sport*. 2017;20:633–637.
9. Schweitzer ME, Karasick D. MR imaging of disorders of the Achilles tendon. *AJR Am J Roentgenol*. 2000;175:613–625.
10. Chang EY, Du J, Chung CB. UTE imaging in the musculoskeletal system. *J Magn Reson Imaging*. 2015;41:870–883.
11. Bydder GM. Review. The Agfa Mayneord lecture: MRI of short and ultrashort T_2 and T_2* components of tissues, fluids and materials using clinical systems. *Br J Radiol*. 2011;84:1067–1082.
12. Han M, Larson PE, Liu J, et al. Depiction of achilles tendon microstructure in vivo using high-resolution 3-dimensional ultrashort echo-time magnetic resonance imaging at 7 T. *Invest Radiol*. 2014;49:339–345.
13. Juras V, Apprich S, Szomolanyi P, et al. Bi-exponential T2 analysis of healthy and diseased Achilles tendons: an in vivo preliminary magnetic resonance study and correlation with clinical score. *Eur Radiol*. 2013;23:2814–2822.
14. Deligianni X, Bar P, Scheffler K, et al. High-resolution Fourier-encoded submillisecond echo time musculoskeletal imaging at 3 Tesla and 7 Tesla. *Magn Reson Med*. 2013;70:1434–1439.
15. Chang EY, Du J, Iwasaki K, et al. Single- and Bi-component T2* analysis of tendon before and during tensile loading, using UTE sequences. *J Magn Reson Imaging*. 2015;42:114–120.
16. Springer F, Steidle G, Martirosian P, et al. Rapid assessment of longitudinal relaxation time in materials and tissues with extremely fast signal decay using UTE sequences and the variable flip angle method. *Invest Radiol*. 2011;46:610–617.
17. Andreisek G, Weiger M. T2* mapping of articular cartilage: current status of research and first clinical applications. *Invest Radiol*. 2014;49:57–62.
18. Scholz TD, Fleagle SR, Burns TL, et al. Tissue determinants of nuclear magnetic resonance relaxation times. Effect of water and collagen content in muscle and tendon. *Invest Radiol*. 1989;24:893–898.
19. Marik W, Nemec SF, Zbyn S, et al. Changes in cartilage and tendon composition of patients with type I diabetes mellitus: identification by quantitative sodium magnetic resonance imaging at 7 T. *Invest Radiol*. 2016;51:266–272.
20. Cook JL, Rio E, Purdam CR, et al. Revisiting the continuum model of tendon pathology: what is its merit in clinical practice and research? *Br J Sports Med*. 2016;50:1187–1191.
21. Fessel G, Wernli J, Li Y, et al. Exogenous collagen cross-linking recovers tendon functional integrity in an experimental model of partial tear. *J Orthop Res*. 2012;30:973–981.
22. Gautieri A, Passini FS, Silvan U, et al. Advanced glycation end-products: mechanics of aged collagen from molecule to tissue. *Matrix Biol*. 2017;59:95–108.
23. Oryan A, Goodship AE, Silver IA. Response of a collagenase-induced tendon injury to treatment with a polysulphated glycosaminoglycan (Adequan). *Connect Tissue Res*. 2008;49:351–360.
24. Vergari C, Pourcelot P, Holden L, et al. A linear laser scanner to measure cross-sectional shape and area of biological specimens during mechanical testing. *J Biomech Eng*. 2010;132:105001.
25. Fessel G, Cadby J, Wunderli S, et al. Dose- and time-dependent effects of genipin crosslinking on cell viability and tissue mechanics—toward clinical application for tendon repair. *Acta Biomater*. 2014;10:1897–1906.
26. Sundararaghavan HG, Monteiro GA, Lapin NA, et al. Genipin-induced changes in collagen gels: correlation of mechanical properties to fluorescence. *J Biomed Mater Res A*. 2008;87:308–320.
27. Almog J, Cohen Y, Azoury M, et al. Genipin—a novel fingerprint reagent with colorimetric and fluorogenic activity. *J Forensic Sci*. 2004;49:255–257.
28. Camenzind RS, Wieser K, Fessel G, et al. Tendon collagen crosslinking offers potential to improve suture pullout in rotator cuff repair: an ex vivo sheep study. *Clin Orthop Relat Res*. 2016;474:1778–1785.
29. de Cesar Netto C, Godoy-Santos AL, Augusto Pontin P, et al. Novel animal model for Achilles tendinopathy: controlled experimental study of serial injections of collagenase in rabbits. *PLoS One*. 2018;13:e0192769.
30. Yeh CL, Kuo PL, Gennisson JL, et al. Shear wave measurements for evaluation of tendon diseases. *IEEE Trans Ultrason Ferroelectr Freq Control*. 2016;63:1906–1921.
31. Perucca Orfei C, Lovati AB, Vigano M, et al. Dose-related and time-dependent development of collagenase-induced tendinopathy in rats. *PLoS One*. 2016;11:e0161590.
32. Robson MD, Bydder GM. Clinical ultrashort echo time imaging of bone and other connective tissues. *NMR Biomed*. 2006;19:765–780.
33. Grosse U, Springer F, Hein T, et al. Influence of physical activity on T1 and T2* relaxation times of healthy Achilles tendons at 3T. *J Magn Reson Imaging*. 2015;41:193–201.
34. Du J, Diaz E, Carl M, et al. Ultrashort echo time imaging with bicomponent analysis. *Magn Reson Med*. 2012;67:645–649.
35. Zheng S, Xia Y. Effect of phosphate electrolyte buffer on the dynamics of water in tendon and cartilage. *NMR Biomed*. 2009;22:158–164.
36. Chang EY, Du J, Bae WC, et al. Effects of Achilles tendon immersion in saline and perfluorochemicals on T2 and T2*. *J Magn Reson Imaging*. 2014;40:496–500.
37. Sein ML, Walton J, Linklater J, et al. Reliability of MRI assessment of supraspinatus tendinopathy. *Br J Sports Med*. 2007;41:e9.
38. Beveridge JE, Machan JT, Walsh EG, et al. Magnetic resonance measurements of tissue quantity and quality using T2 * relaxometry predict temporal changes in the biomechanical properties of the healing ACL. *J Orthop Res*. 2017.
39. Wilson KJ, Surowiec RK, Johnson NS, et al. T2* mapping of peroneal tendons using clinically relevant subregions in an asymptomatic population. *Foot Ankle Int*. 2017;38:677–6783.
40. Krepkin K, Bruno M, Raya JG, et al. Quantitative assessment of the supraspinatus tendon on MRI using T2/T2* mapping and shear-wave ultrasound elastography: a pilot study. *Skeletal Radiol*. 2017;46:191–199.
41. Tourell MC, Momot KI. Molecular dynamics of a hydrated collagen peptide: insights into rotational motion and residence times of single-water bridges in collagen. *J Phys Chem B*. 2016;120:12432–12443.
42. Peto S, Gillis P, Henri VP. Structure and dynamics of water in tendon from NMR relaxation measurements. *Biophys J*. 1990;57:71–84.
43. Fullerton GD, Rahal A. Collagen structure: the molecular source of the tendon magic angle effect. *J Magn Reson Imaging*. 2007;25:345–361.
44. Xia Y. Magic-angle effect in magnetic resonance imaging of articular cartilage: a review. *Invest Radiol*. 2000;35:602–621.

45. Camenzind RS, Tondelli TO, Gotschi T, et al. Can genipin-coated sutures deliver a collagen crosslinking agent to improve suture pullout in degenerated tendon? An ex vivo animal study. *Clin Orthop Relat Res*. 2018;476:1104–1113.

46. Silver IA, Brown PN, Goodship AE, et al. A clinical and experimental study of tendon injury, healing and treatment in the horse. *Equine Vet J Suppl*. 1983;1–43.

47. Juras V, Zbyn S, Pressl C, et al. Regional variations of T_2* in healthy and pathologic achilles tendon in vivo at 7 Tesla: preliminary results. *Magn Reson Med*. 2012;68:1607–1613.

48. Robson MD, Benjamin M, Gishen P, et al. Magnetic resonance imaging of the Achilles tendon using ultrashort TE (UTE) pulse sequences. *Clin Radiol*. 2004;59:727–735.

49. Diaz E, Chung CB, Bae WC, et al. Ultrashort echo time spectroscopic imaging (UTESI): an efficient method for quantifying bound and free water. *NMR Biomed*. 2012;25:161–168.

50. Snedeker JG, Foolen J. Tendon injury and repair—a perspective on the basic mechanisms of tendon disease and future clinical therapy. *Acta Biomater*. 2017;63:18–36.

51. Reeves ND, Cooper G. Is human Achilles tendon deformation greater in regions where cross-sectional area is smaller? *J Exp Biol*. 2017;220(Pt 9):1634–1642.